A Simple Printed Dipole Antenna with Broadband Characteristics

Tuan Hung Nguyen
Faculty of Radio-Electronic Engineering
Le Quy Don Technical University
Hanoi, Vietnam
hungnt1985_k31@lqdtu.edu.vn

Itsuki Sasaki
Department of Electrical and Electronic Engineering
National Defense Academy
Yokosuka, Japan
f19003@nda.ac.jp

Yuta Nakagawa
Department of Electrical and Electronic Engineering
National Defense Academy
Yokosuka, Japan
ed18002@nda.ac.jp

Hisashi Morishita
Department of Electrical and Electronic Engineering
National Defense Academy
Yokosuka, Japan
morisita@nda.ac.jp

Abstract— **This paper presents a microstrip-fed printed dipole antenna (PDA) which can cover a wide frequency band (roughly 80% for $|S_{11}| < $ -6 dB), and maintain the omnidirectional radiation patterns in the entire operation band. The antenna shape is very simple. Two identical arms of the antenna upon two sides of an FR-4 substrate are placed inversely to each other and their shapes are similar to that of an inset-fed rectangular patch antenna. Our results show that the proposed antenna is very capable for many applications of small antennas while it has the compact size of $0.3\lambda \times 0.008\lambda$ at the minimum operation frequency of $|S_{11}| = $ -6 dB.**

Keywords— *printed dipole antenna, broadband characteristic, omnidirectional radiation pattern.*

I. INTRODUCTION

Dipole is one of the most fundamental antennas which has been widely studied in theory and applied in practice [1]. Various types of dipole including printed dipole, have been popular and investigated in many works [2]-[6]. Regarding printed dipoles, their most unique feature in these works is that their structures are simply composed of two arms printed on two sides of a dielectric substrate, and their resonant bandwidths are often maximized by properly adjusting these arms. Beside the advantage of resonant bandwidth improvement, however, each antenna has one or more disadvantages, such like the requirement of using a balun [2]-[4], or the degradation of omnidirectional radiation patterns [3], [5], or the large number of dimension parameters that need to be optimized [2]-[6]. In this study, we introduce a unique structure of printed dipole antenna which can relatively overcome these disadvantages and provide broadband property in both impedance and radiation pattern.

II. PROPOSED ANTENNA CONFIGURATION

Side, top, and bottom views of the proposed antenna are shown in Fig. 1. This antenna also has two arms with each arm printed upon one side of a rectangular FR-4 substrate. The substrate size is 120 × 33 mm with the thickness of 1 mm, relative permittivity of $\varepsilon_r = 4.8$, and loss tangent of $\tan\delta = 0.019$. The two arms are identical to each other, and similar to the shape of a microstrip inset-fed patch described in Chapter 14 of [1]. Each arm is composed of a "patch" part (60 × 33 mm) and a "line" part (60 × 1.75 mm). In CST simulation, a waveguide port constructed from the "line" part

of the top arm (as a microstrip line) and the "patch" part of the bottom arm (as a ground) is used to fed the antenna. In order to provide a characteristic impedance of $Z_0 = 50$ Ω from the waveguide port, the width of the "line" part of the top arm (Fig. 1(b)) needs to be set to 1.75 mm. On the other hand, there is no necessity to set the width of the "line" part of the bottom arm (Fig. 1(c)) to be 1.75 mm as it is not a feeding line, but for symmetric antenna modeling, it is 1.75 mm, too. Besides, as described later in section II, the length *ls* and the width *ws* of the slots in top and bottom arms are two important parameters in achieving the broadband operation of the proposed antenna.
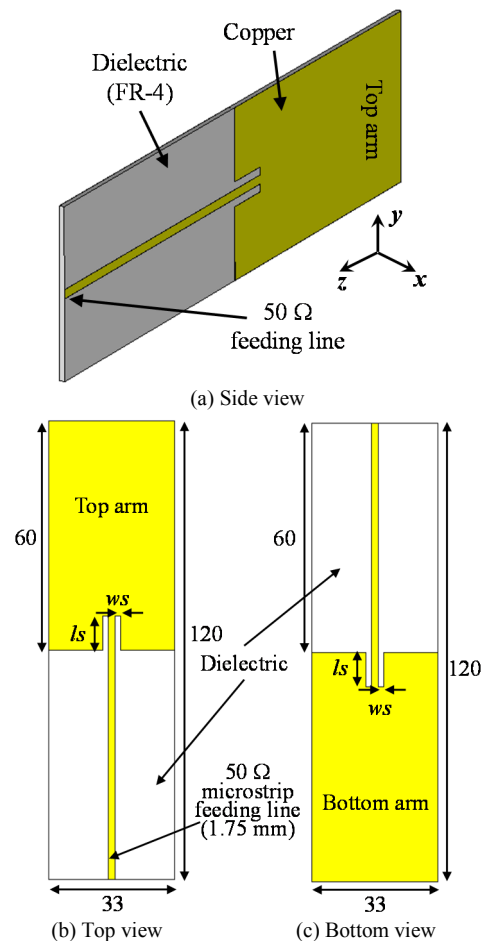

Fig. 1. Configuration of the proposed antenna (*Dimension unit: mm*).

III. BROADBAND CHARACTERISTICS

In turn, we focus on the reflection coefficient and radiation characteristics of the proposed antenna by CST simulations.

A. Reflection coefficient and VSWR

First, in order to clarify the importance of the slots, we investigate the variation of reflection coefficient's magnitude $|S_{11}|$ with different values of slot length ls and slot width ws. For convenience, we use the criterion of $|S_{11}| < -6$ dB to evaluate the input impedance bandwidth in this study.

Figure 2 shows the variation of $|S_{11}|$ when fixing the slot width ws to 1.5 mm, and changing the slot length ls. The initial antenna shape is that with no "inset-fed" part (when $ls = 0$ mm or $ws = 0$ mm). In this case, the $|S_{11}|$ of the antenna is the thin green solid curve shown in Fig. 2, and the fractional bandwidth for $|S_{11}| < -6$ dB is about 39% (0.844-1.254 GHz) with only one resonance near 0.98 GHz. As indicated by the thin blue dashed curve in Fig. 2, when ls is increased to 5 mm, the appearance of two resonances at around 0.87 GHz and 1.1 GHz with better impedance matching can be observed, and this extends the fractional bandwidth to 52% (0.8-1.362 GHz). Also in Fig. 2, the fractional bandwidth keeps widening if ls is increased to 9 mm as shown by the thick red solid curve. When $ls = 9$ mm, a third resonance appears at 1.7 GHz beside the 1st (0.81 GHz) and 2nd (1.19 GHz) ones, and in this case, the fractional bandwidth is extended to roughly 80% (0.76-1.76 GHz).
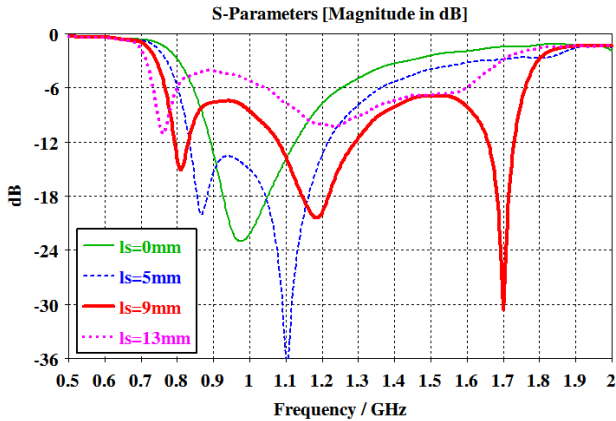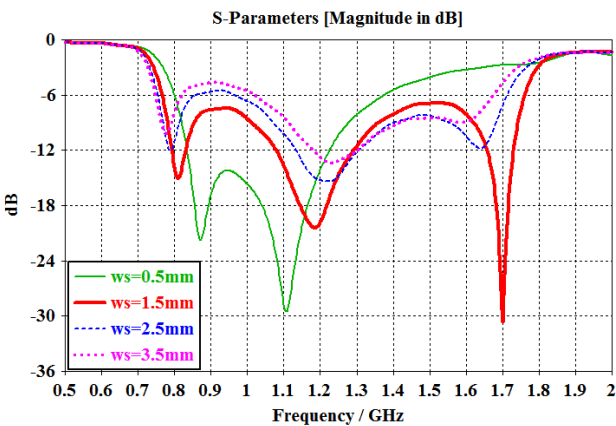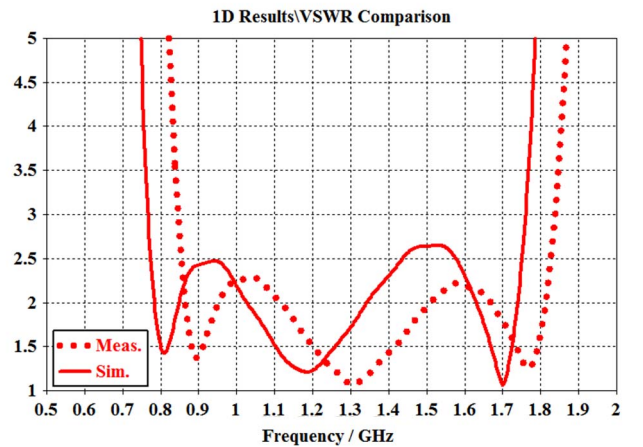
However, when ls exceeds 9 mm, for example, $ls = 13$ mm as the thin pink dotted curve in Fig. 2, impedance matching in the band between the 1st and 2nd resonances begins to deteriorate, and broadband property is no longer available. Hence, in this investigation, it is clear that when ws is fixed to 1.5 mm, the most adequate value of ls to obtain the widest fractional bandwidth of the antenna is 9 mm.

Similarly, in Fig. 3, we investigate the variation of $|S_{11}|$ when fixing the slot length ls to 9 mm and changing the slot width ws. As shown by the thin green solid curve in Fig. 3, the very small value of ws like $ws = 0.5$ mm will make the 3rd resonance totally disappear, and the bandwidth shrinks despite the slight improvement of impedance matching between the two remaining resonances. In this case, we observe that the thin green solid curve in Fig. 3 has a relatively similar trend to that of the thin blue dashed curve in Fig. 2. The reason of this similarity can be considered that the currents inducing around the edges of each slot in the case of $ls = 5$ mm, $ws = 1.5$ mm (thin blue dashed curve in Fig. 2) and in the case of $ls = 5$ mm, $ws = 1.5$ mm (thin green solid curve in Fig. 3) have the same effects on antenna's input impedance. On the other hand, as in the cases of $ws = 2.5$ mm and 3.5 mm resulted in Fig. 3, when the slot width ws is larger than 1.5 mm, values of $|S_{11}|$ around 0.92 GHz increase, and certainly, the broadband characteristic of the antenna is not maintained. Therefore, in this investigation, it is also clear that, in order to obtain the widest bandwidth when $ls = 9$ mm, the value of ws needs to be set to 1.5 mm.

Although we do not implement any optimization process to optimize ls and ws in this study, from the results of two investigations above, we can roughly conclude that when other antenna dimension parameters are fixed as in Fig. 1,

Fig. 2. Variation of $|S_{11}|$ when changing ls.

Fig. 3. Variation of $|S_{11}|$ when changing ws.
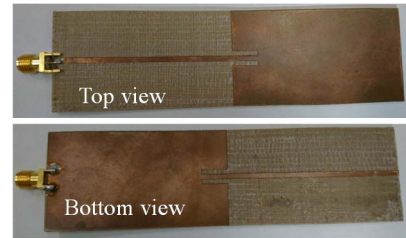
(a) Fabricated antenna

(b) VSWR characteristics

Fig. 4. Fabricated antenna and its measured VSWR characteristic compared to simulation result.

the slot with $ls = 9$ mm and $ws = 1.5$ mm is one of the best factors for maximizing the input impedance bandwidth of the proposed antenna. Certainly, more optimal combinations of ls and ws which can perform the identical broadband property of the antenna may exist, if they can provide the same effect of current distribution on $|S_{11}|$, especially currents induced around slots' edges.

To confirm the broadband property of the proposed antenna, we made a fabrication model and measured its VSWR characteristic by a vector network analyzer as indicated in Fig. 4. In Fig. 4(b), it is obvious that although there is a slight frequency shift of the measured VSWR (dotted curve) compared to the simulated one (solid curve), both of them have the same trend to each other with three resonant frequencies in each curve and wide bandwidths for VSWR < 3 ($|S_{11}| < -6$ dB). The reason of the frequency shift between measurement and simulation results may be the difference in relative permittivity of the dielectric substrate between fabricated and simulated models.

B. Radiation pattern

In this part, we investigate radiation characteristics of the proposed antenna configuration which has $ls = 9$ mm and $ws = 1.5$ mm. The investigation focuses on the radiation patterns at three resonant frequencies of $f_1 = 0.81$ GHz, $f_2 = 1.19$ GHz, and $f_3 = 1.7$ GHz. The simulated results of radiation patterns at these frequencies in xy-plane ($\theta = 90°$; $0° \leq \phi \leq 360°$) and xz-plane ($\phi = 0°$; $0° \leq \theta \leq 180°$) are respectively shown in Fig. 5 (a) and (b). In each graph, realized gains including input matching loss are plotted in dBi unit. Besides, in both graphs, since the E_ϕ component is very small, only the E_θ component is plotted.

From Fig. 5(a), we can easily see that in xy-plane, the proposed antenna has omnidirectional patterns at $f_1 = 0.81$ GHz and $f_2 = 1.19$ GHz, and nearly omnidirectional pattern at $f_3 = 1.7$ GHz. In xz-plane, the proposed antenna shows the radiation patterns of "8" shape at all resonant frequencies. These results reveal that the radiation patterns of the proposed antenna are very similar to those of a typical wire dipole antenna [1]. To prove this issue, we implement a further comparison on radiation patterns of the proposed antenna and a wire dipole antenna as below.

As depicted in [1], a thin wire dipole antenna (wire diameter is about 0) which has the length l along z-axis yields a radiation pattern expressed by:

$$F(\theta, \phi) = F(\theta) = \left[\frac{\cos\left(\frac{kl}{2}\cos\theta\right) - \cos\left(\frac{kl}{2}\right)}{\sin\theta} \right]^2 \quad (1)$$

And its maximum directivity D_0 is:

$$D_0 = \frac{2F(\theta)\big|_{max}}{\int_0^\pi F(\theta)\sin\theta \, d\theta} \quad (2)$$

Table I summarizes half-power beamwidth (*HPBW*) and maximum directivity D_0 of both the wire dipole antenna and the proposed antenna. *HPBW* and D_0 of the wire dipole antenna are calculated with different values of length l ($l = \lambda/4$, $\lambda/2$, and $3\lambda/4$) from equations (1) and (2), while those of the proposed antenna are derived in CST simulation at three
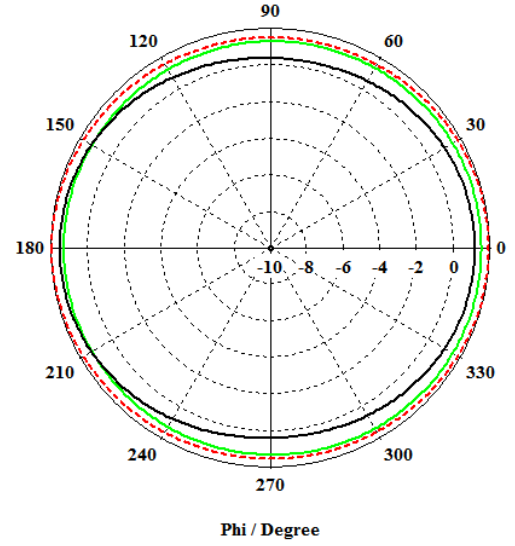
(a) *xy*-plane
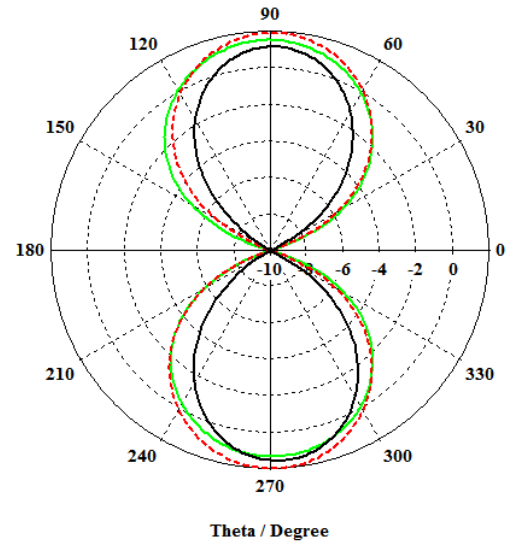
(b) *xz*-plane

—— $f_1 = 0.81$ GHz   - - - - $f_2 = 1.19$ GHz   —— $f_3 = 1.7$ GHz

Fig. 5. Simulated realized gain radiation pattern of the proposed antenna at 3 resonant frequencies when $ls = 9$ mm and $ws = 1.5$ mm (*Unit: dBi*).

TABLE I.   COMPARISON BETWEEN PROPOSED ANTENNA AND WIRE DIPOLE ANTENNA

Half-power beamwidth (*HPBW*)			
Wire dipole antenna	$l = \lambda/4$	$l = \lambda/2$	$l = 3\lambda/4$
	87°	78°	64°
Proposed antenna	f_1	f_2	f_3
	84.4°	77.2°	65.7°
Maximum directivity (D_0 - dimensionless)			
Wire dipole antenna	$l = \lambda/4$	$l = \lambda/2$	$l = 3\lambda/4$
	1.53	1.67	1.92
Proposed antenna	f_1	f_2	f_3
	1.67	1.77	2.15

resonant frequencies.

It is easy to confirm in Table I that the two antennas have very close values to each other both in *HPBW* and D_0. These results show that the proposed antenna operates like a $\lambda/4$ wire dipole at its 1st resonant frequency f_1, like a $\lambda/2$ wire

TABLE II. COMPARISON BETWEEN PROPOSED ANTENNA AND THE OTHERS IN REFERENCES

	Size at f_{min} of |S_{11}| = -6 dB	Fractional bandwidth (|S_{11}| < -6 dB)	Balun need	Radiation patterns
Antenna in [2]	$0.35\lambda \times 0.03\lambda$	55%	Yes	Omnidirectional at 2 resonances
Antenna in [3]	$0.52\lambda \times 0.1\lambda$	77%	Yes	Nearly omnidirectional at 2 resonances
Antenna in [4]	$0.4\lambda \times 0.2\lambda$	43%	Yes	Omnidirectional at 2 resonance
Antenna in [5]	$0.64\lambda \times 0.12\lambda$	> 100%	No	Directional in all band
Antenna in [6]	$0.38\lambda \times 0.38\lambda$	28% + 21%	No	Omnidirectional at 2 resonances
Our proposed antenna	$0.3\lambda \times 0.08\lambda$	80%	No	Omnidirectional at 3 resonances

dipole at its 2nd resonant frequency f_2, and like a $3\lambda/4$ wire dipole at its 3rd resonant frequency f_3. This is a very interesting and unique feature of the proposed antenna that the others [2]-[6] do not have, as it can maintain the conventional radiation pattern of dipole in the entire resonant frequency band. That is to say, the proposed antenna has broadband properties not only in input impedance but also in radiation characteristics.

To compare more in details the proposed antenna with the others in [2]-[6], we show the statistical data of all these antennas in Table II including antenna size (normalized at the minimum operation frequency of \|S_{11}\| = -6 dB in each case), fractional bandwidth (\|S_{11}\| < -6 dB), the nessecity of using a balun, and the shapes of radiation patterns at resonant frequencies of each antenna. The data clearly denote the helpful advantages of the proposed antenna, that although it has the smallest normalized size, it still provide a very wide fractional bandwidth and omnidirectional radiation pattern at all 3 resonant frequencies without using a balun.

IV. CONCLUSION

In this work, a simple and broadband printed dipole antenna has been proposed and investigated. The results show that the proposed antenna is very capable for application of small antennas because it has a compact size, and can cover roughly 80% fractional bandwidth (\|S_{11}\| < -6 dB) with easy microstrip feeding structure, and moreover, maintain the omnidirectional radiation pattern of dipole antenna in the whole band. In future works, detailed analysis on the antenna characteristics will be implemented to clarify the operation mechanism of this antenna.

REFERENCES

[1] C. A. Balanis, Antenna theory analysis and design, 3rd ed., John Wiley & Sons Inc., New Jersey, 2005.

[2] Y. W. Chi, K. L. Wong, and S. W. Su, "Broadband Printed Dipole Antenna With a Step-Shaped Feed Gap for DTV Signal Reception," IEEE Trans. Antennas Propag., vol. 55, no. 11, pp. 3353–3356, Nov. 2007.

[3] A. R. Behera, and A. R. Harish, "A Novel Printed Wideband Dipole Antenna," IEEE Trans. Antennas Propag., vol. 60, no. 9, pp. 4418–4422, Sept. 2012.

[4] M. Nagatoshi, S. Tanaka, S. Horiuchi, and H. Morishita, "Broadband characteristics of a planar folded dipole antenna with a feed line," IEICE Trans. Commun. vol. E94-B, no. 5, pp. 1168-1173, May 2011.

[5] D. T. Le, Q. D. Nguyen, and Y. Karasawa, "A New Scheme to Enhance Bandwidth of Printed Dipole for Wideband Applications," IEICE Trans. Commun., vol. E97-B, no. 4, pp. 773-782, April 2014.

[6] P. Wu, Z. Kuai, and X. Zhu, "Multiband Antennas Comprising Multiple Frame-Printed Dipoles," IEEE Trans. Antennas Propag., vol. 57, no. 10, pp. 3313–3316, Oct. 2009.